The Polymer Physics of Multiscale Charge Transport in Conjugated Systems

Kaichen Gu,[1] Yueh-Lin Loo [1,2]

[1]Department of Chemical and Biological Engineering, Princeton University, Princeton, New Jersey, 08544
[2]Andlinger Center for Energy and the Environment, Princeton University, Princeton, New Jersey, 08544
Correspondence to: K. Gu (E-mail: kaicheng@princeton.edu) and Y.-L. Loo (E-mail: lloo@princeton.edu)

Received 30 May 2019; revised 4 August 2019; accepted 5 August 2019; published online 16 August 2019
DOI: 10.1002/polb.24873

ABSTRACT: Conjugated polymers are promising candidates for next-generation low-cost flexible electronics. Field-effect transistors comprising conjugated polymers have witnessed significant improvements in device performance, notably the field-effect mobility, in the last three decades. However, to truly make these materials commercially competitive, a better understanding of charge-transport mechanisms in these structurally heterogeneous systems is needed for providing systematic guides for further improvements. This review assesses the key microstructural features of conjugated polymers across multiple length scales that can influence charge transport, with special attention given to the underlying polymer physics. The mechanistic understanding from collective experimental and theoretical studies point to the importance of interconnected ordered domains given the macromolecular nature of the polymeric semiconductors. Based on the criterion, optimization to improve charge transport can be broadly characterized by efforts to (a) promote intrachain transport, (b) establish intercrystallite connectivity, and (c) enhance interchain coupling. © 2019 Wiley Periodicals, Inc. J. Polym. Sci., Part B: Polym. Phys. **2019**, *57*, 1559–1571

KEYWORDS: chain conformations; charge transport; conjugated polymers; organic electronics; polymer physics; structure–property relationship

INTRODUCTION Conjugated polymers are promising electrically active components in flexible large-area electronic devices that can be fabricated in a low-cost and high-throughput fasion.[1–4] The joint efforts of physicists, engineers, and chemists have led to remarkable improvements in the performance of these devices. In this review, we will focus on polymer thin-film transistors, whose performance has seen stunning progress over the last three decades. Thin-film transistors are not only fundamental building blocks for modern electrical circuits but also the most common device platform from which charge-transport physics can be extracted. Because the demonstration of the first polymer field-effect transistors in 1986,[5] the field-effect mobility (μ), a metric by which transistor performance is primarily evaluated, has steadily increased from $\sim 10^{-5}$ to ~ 10 cm^2 V^{-1} s^{-1}, exceeding the benchmark that is set by their amorphous silicon counterparts.[6–11] Continuous improvements of device performance through iterative refinement of materials design and optimization of processing techniques and conditions are coupled with concomitant developments of our understanding about the underlying charge-transport mechanisms. Research efforts to enhance charge transport in conjugated polymers initially focused on increasing their long-range order and crystallinity. The purported need for long-range order and high crystallinity led to the advancements in synthetic techniques, which yielded polythiophenes with high regioregularity. It follows that regioregular poly(3-hexylthiophene), or P3HT, has become the most ubiquitous and widely studied conjugated polymer, whose transistors routinely exhibit mobilities above 0.01 cm^2 V^{-1} s^{-1}, a great improvement compared to prior transistors based on amorphous regiorandom polythiophenes having mobilities of 10^{-5} to 10^{-4} cm^2 V^{-1} s^{-1}.[1,12] The requirement for high crystallinity to support efficient charge transport subsequently led to the design of a yet-more crystalline polythiophene derivative, poly(bithiophene-*alt*-thienothiophene), or PBTTT, whose transistors showed then-record-setting mobilities above 0.1 cm^2 V^{-1} s^{-1}.[1,13] However, recent reports of high-performance transistors (with mobilities above 1 cm^2 V^{-1} s^{-1}, some even above 10 cm^2 V^{-1} s^{-1}) based on donor–acceptor copolymers that exhibit limited long-range order have called into question crystallinity as the sole governing parameter for efficient charge transport and implicate interconnectivity between crystalline aggregates as an equally important parameter.[14,15]

Many theoretical tools and frameworks have been developed to describe how the single-chain characteristics and microstructure in melts and solid states impact the bulk mechanical properties of commodity polymers.[16] We argue that these tools and frameworks can also lend insight to charge transport in conjugated polymers because there can be a common

Kaichen Gu received his B.A. and M.Eng. in Chemical Engineering from the University of Cambridge in 2015. He is currently a Ph.D. candidate, advised by Prof. Yueh-Lin Loo, in the Department of Chemical and Biological Engineering at Princeton University. His research work focuses on the elucidation of charge-transport mechanisms in semiconducting conjugated polymer thin films.

Yueh-Lin Loo is the Theodora D. '78 and Willliam H. Walton III '74 Professor in Engineering and director of the Andlinger Center for Energy and the Environment at Princeton University. Her group is interested in the processing and structural development of materials for lightweight and flexible solar cells and circuits, the combination is explored for self-powered "smart" windows to increase occupant comfort, building and energy efficiencies. She is a Fellow of the American Physical Society.

microstructural origin for mechanical and electrical properties.[17] For example, moderately crystalline P3HT is more flexible and ductile than highly crystalline PBTTT. The field-effect mobility ratio of transistors comprising these two polymers is very similar to their elastic modulus ratio, shown in Figure 1.[18] In light of the success in engineering desired mechanical properties of polyolefins, we believe that many opportunities exist not only to establish empirical correlations between mechanical and electrical properties, like the mobility–modulus relationship mentioned above, but also to shed light on the underlying structural origin and polymer physics for charge transport.[17] This review highlights how these ideas and frameworks have been leveraged—and in some other cases extended—to gain insights on how polymer microstructure impacts charge transport in conjugated polymers. For instance, long polymer chains have

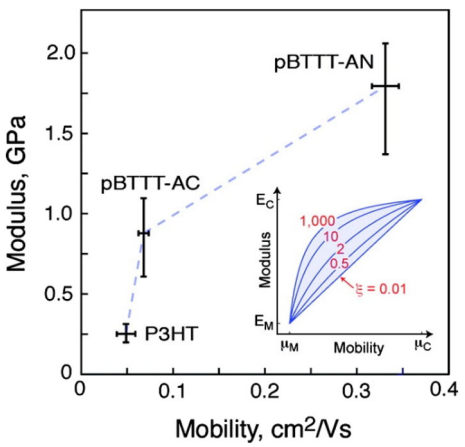

FIGURE 1 Comparison of the field effect mobility and elastic modulus of P3HT, as-cast pBTTT (pBTTT-AC), and annealed pBTTT (pBTTT-AN) films. Inset, the mobility and elastic modulus of a semicrystalline polymer with increasing percent crystallinity, based on composite theories of charge transport and elastic modulus with two distinct values for the amorphous (μ_M, E_M) and crystalline (μ_C, E_C) portions of the films. Reprinted with permission from (*ACS Nano* **2010**, *4*, 7538–7544). Copyright (2010) American Chemical Society.

the ability of bridging adjacent crystallites; such chains are known as polymer tie chains. The presence of tie chains strongly influences the resistance to slow crack growth in polyethylene resins.[19,20] By extension, the presence of tie chains that connect neighboring crystallites has been recently shown to also play a critical role on charge transport in P3HT. Although direct visualization of tie chains remains challenging, this extension allows estimation of tie-chain fraction in P3HT, establishing the concept of a critical threshold of tie-chain connectivity that is required for macroscopic charge transport in P3HT.[21]

In this review, we aim to assess the polymer physics of multiscale charge transport in conjugated systems. We first describe the microstructural features of conjugated polymers across multiple length scales that can influence charge transport. We then assess a plethora of literature that has examined the structure–electrical property relationships of conjugated polymers, highlighting both empirical and theoretical studies aimed at identifying the governing molecular characteristics and structural features for charge transport. We seek to draw insights from these collective studies to understand the underlying charge-transport mechanisms in such complex systems and propose design rules accordingly. Although there exist transistors comprising many other more exotic polymers whose mobilities are higher than those of P3HT transistors, the abundance of literature on this model polymer system allows for a more in-depth analysis of structure–property relationships. Many important physical parameters, which are not available for most other conjugated polymers, have been characterized for P3HT, including its persistence length (3 nm),[22] monomer length (0.39 nm),[23] equilibrium melting temperature (272 °C),[24,25] and enthalpy of fusion of a perfect crystal (49 J g^{-1}),[25] and so on. As a result, much of our discussion will be focused on P3HT. Nonetheless, we point out differences between P3HT and other conjugated polymers where appropriate. Finally, we discuss materials design rules and processing guidelines that have surfaced from these collective works for improving charge transport and propose opportunities for further progress. This review focuses on charge transport in homopolymers. We refer the readers to other reviews for a comprehensive discussion of polymer blends and block copolymers explored for their

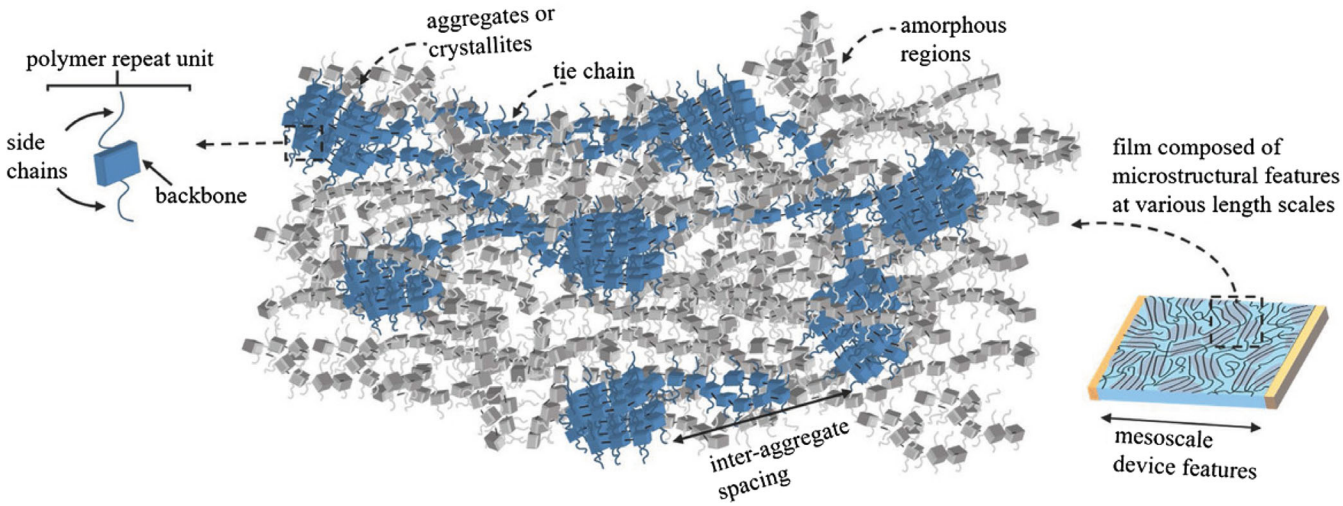

FIGURE 2 Cartoon representation of typical microstructure of conjugated polymers.[29] The polymer thin film comprises both ordered and amorphous regions, which are typically much smaller than the device dimension. The ordered domain can be made up of either aggregates or crystallites. Polymer tie chains provide the connectivity between the ordered domains. Reprinted with permission from (*Macromol. Rapid Commun.* **2018**, *39*, 1–9). Copyright (2018) John Wiley & Sons, Inc.

optoelectronic applications.[26–28] Polymer systems with multiple components or complex architectures bring added complexity, stemming from the need to understand their mixing behavior at different length scales, that are beyond the scope of this review.

MULTISCALE CHARGE TRANSPORT IN CPS

Polymer chains have many degrees of conformational freedom and interact with each other *via* weak van der Waals forces, which lead to a complex and sometimes kinetically trapped solid-state microstructure, hampering the elucidation of charge-transport mechanisms. Although the impacts of structural features at different length scales on charge transport are often convoluted, it is prerequisite to first understand the hierarchical structure of typical conjugated polymers. The cartoon representation in Figure 2 highlights the salient microstructural features present at the mesoscale dimension of a device. The polymer active layer comprises both ordered and amorphous regions. The ordered domains can be made up of either aggregates or crystallites. For P3HT, Duong *et al*. made the following distinction between the two species: an aggregate exhibits order in the π-stacking direction whereas a crystallite, composed of alkyl-stacked aggregates, exhibits additional order in the alkyl-stacking direction. Hence, a crystallite contains aggregates, but not all aggregates form crystallites.[30] Generally, X-ray diffraction and calorimetric techniques are applied to probe crystallites, whereas only optical measurements are used to investigate aggregates,[31] because some aggregates contain very few π-conjugated segments that can often be too small to exhibit discernible Bragg diffraction.[30,31] Charge transport in conjugated polymers is largely determined by π-orbital overlap and electron delocalization. Charge transport within crystallites can thus be highly anisotropic; it is the fastest along the conjugated polymer backbone, next fastest along the π-stacking direction, and essentially absent in the direction of side-chain stacking.[32,33] In order for macroscopic charge transport to be efficient, neighboring crystallites need to be connected so inter-crystallite transport can take place. Individual chains that span two neighboring crystallites form tie chains to provide connectivity between adjacent ordered domains. The formation of tie chains is dependent on single-chain characteristics, including chain rigidity and length, as well as the processing conditions, which critically impact structural parameters, including the size and fraction of ordered regions and the separation between them.[21,31]

The hierarchical structure in these materials in turn leads to a multiscale charge-transport process. At characteristic lengths comparable to the persistence length of the conjugated polymer (typically a few nanometers), charges can move efficiently along the polymer backbone. Charge transport at this length scale is dictated by intrachain electronic coupling between connected mers. At lengths comparable to the size of polymer aggregates or crystallites (typically 10's of nanometer), charge transport is dictated by interchain electronic coupling and requires multiple interchain hopping events, which is typically two or three orders of magnitude slower than intrachain charge transport. At longer yet length scales (above 100's of nanometer; typical transistor channel lengths are well above 1 μm), macroscopic charge transport is limited by transport in the amorphous regions where π-stacking is disrupted, unless the ordered domains are sufficiently connected, in which case charge transport is then limited by the interchain hopping within the ordered regions.[29,34,35]

Bridging the gaps in our knowledge about microstructures across length scales and our interest in macroscopic charge transport and, ultimately device performance, will facilitate the deployment of morphologically heterogeneous conjugated polymers in large-scale opto-electronic applications.[15,36,37]

POLYMER CHAIN CONFORMATIONS

One of the starting points to understanding the underlying physics in conjugated polymers is to probe their chain conformations, that is, the spatial configurations of constitutive mers along a polymer chain,[28] which provide the underlying molecular basis of almost all their physical properties.[38] The electronic properties of conjugated polymers and thus the performance of devices comprising them are also strongly dependent on their chain conformations.[39–41] Conjugated polymers are typically semiflexible. Polymer chains that have more flexible backbones, and those with more defects thus generally have reduced effective conjugation lengths, which increase their propensity to trap charge carriers and hence lower overall device performance when incorporated in transistors.[15]

Polymer chain rigidity is quantified by its persistence length (L_p), which is mathematically defined by the decay length of the tangent–tangent angular orientational correlations along the chain.[42] Persistence length is an important dimensional characteristic; it defines the regimes across which theoretical treatments of chain conformations differ. When the contour length (L_c), the length of a chain at its maximum physical extension, is much larger than L_p, the polymer behaves like a flexible chain, which is modeled with a random walk of Kuhn segments of length l_k ($l_k = 2L_p$). When L_c of a chain is instead much smaller than L_p, the polymer chain is treated as a rigid rod. In the intermediate regime when L_c is comparable to L_p, the semiflexible chain is described by a worm-like chain (WLC) model.[42,43]

Experimentally, the persistence length of conjugated polymers can be estimated by viscometry,[44] light scattering,[44,45] small-angle neutron scattering (SANS),[22] and diffusion-ordered NMR spectroscopy (DOSY).[46] Using SANS, McCulloch *et al*. systematically investigated the factors that impact the chain shape of poly(3-alkylthiophenes), P3ATs, and found the chain rigidity of conjugated polymers to be sensitive to side-chain chemistry, regioregularity, and the presence of defects along the backbone introduced during synthesis, detailed in Figure 3.[22]

Alternatively, the persistence length can be computed *via* molecular dynamics (MD) simulations,[47] but full atomistic simulations require the development of appropriate force fields and can be computationally expensive.[28,43] Complicating such endeavors is the limited availability of quantitative structural information on conjugated polymers beyond P3HT.[28] In a simplified version, Zhang *et al*. estimated the persistence length of P3HT and poly((9,9-dioctylfluorene)-2,7-diyl-*alt*-[4,7-bis(thiophen-5-yl)-2,1,3-benzothiadiazole]-2,2-diyl), or PFTBT, by averaging a large number of chain conformations with a dihedral potential distribution according to the hindered rotation (HR) model.[43] The model estimated the persistence length of P3HT as 4.0 nm, in reasonable agreement with SANS results (3.0 nm). The persistence length of PFTBT was estimated as 5.9 nm, but the corresponding experiment had not been conducted.[43]

The planarity of the polymer chain also plays an important role on charge transport, especially when there are insufficient π–π interactions between neighboring chains to promote the mesoscale ordering needed for effective interchain transport. IDTBT, an indacenodithiophene–benzothiadiazole copolymer, for example, has resulted in transistors with surprisingly high mobilities despite exhibiting very limited long-range order. This unusual finding is attributed to IDTBT having a planar conformation with a largely torsion-free backbone, as demonstrated by quantum chemical and MD calculations, as well as measured by pressure-dependent Raman spectroscopy.[48] This backbone planarity is believed to subsume mesoscale structural disorder, enabling IDTBT to exhibit transport properties approaching intrinsic disorder-free transport limits.[14,48]

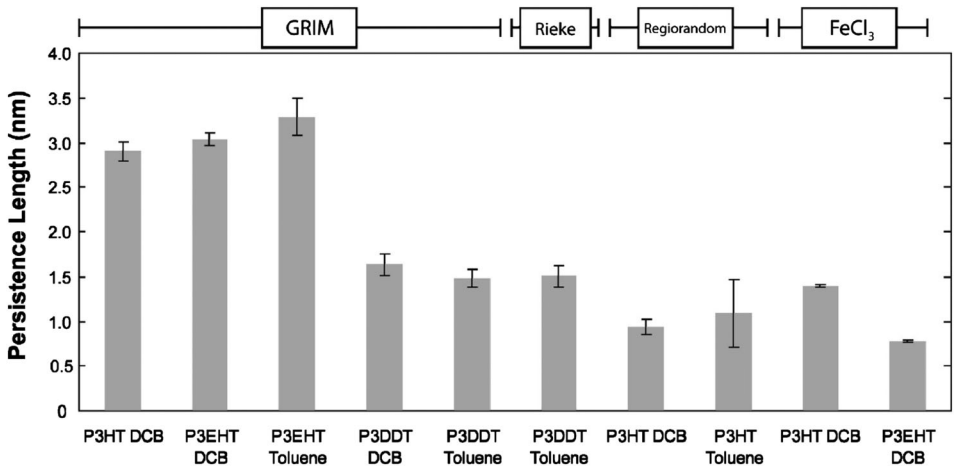

FIGURE 3 Comparison of the persistence length from the wormlike chain model shows how chain rigidity of poly(3-alkylthiophene)s depends on side-chain chemistry and regioregularity.[22] Poly(3-hexylthiophene), P3HT; poly(3-(2-ethyl)hexylthiophene), P3EHT; and poly(3-dodecylthiophene), P3DDT, were synthesized *via* Grignard metathesis polymerization (GRIM). P3HT and P3EHT were also synthesized *via* a $FeCl_3$-catalyzed polymerization. Regiorandom P3HT and Rieke P3DDT were purchased from Sigma-Aldrich. Reprinted with permission from (*Macromolecules* **2013**, *46*, 1899–1907). Copyright (2013) American Chemical Society.

These efforts to experimentally measure or computationally predict the backbone planarity and rigidity have provided the key initial steps to understanding the chain conformation of conjugated polymers. Although a direct and quantitative connection between chain conformation and charge transport remains elusive, it is nonetheless important to understand the chain conformations because they strongly impact the aggregation behavior and interaggregate connectivity, both of which are important to charge transport in conjugated polymers. Intriguingly, recent donor–acceptor polymers that make up the active layers of high-mobility transistors have relatively stiff backbones, possessing much higher persistence lengths than that of the quintessential P3HT.[28]

BRIDGING ELECTRICAL PROPERTIES AND MORPHOLOGY

Structure–Property Relationships

It has been widely established that the mesoscale morphology plays a critical role on charge transport in conjugated polymers. Figure 4a shows the charge propagation processes in regioregular P3HT at different length scales, including intrachain and interchain transport in both the ordered and disordered regions, which occur at different rates.[49] The overall charge transport depends on many structural features, including the size, fraction, and orientation of ordered regions, as well as the interconnectivity between them.[49] The semicrystalline morphology of P3HT was directly visualized by the scanning tunneling microscopy (STM) in Figure 4b.[50] Crystalline domains appear lighter than the disordered or amorphous regions. The crystalline domains appear connected,[50] presumably *via* tie chains that are prevalent in semicrystalline commodity polymers. Such connections, composed of strong covalent bonds, have long been recognized to critically impact the mechanical properties of polyolefin resins.[20] Without these connections, crystallites would be held together by weak van der Waals or hydrogen bonds, leading to macroscopic brittleness.[20] In analogy to how tie chains impact mechanical properties, tie chains should provide connective pathways between ordered domains in conjugated systems. In support of this assertion, Noriega *et al.* argued that the presence of interconnected ordered domains is the unifying requirement for macroscopic charge transport.[15]

Achieving an interconnected network of ordered domains in the active layer to realize high electrical performance requires both optimal materials design and control over processing conditions. Figure 5 summarizes the intrinsic properties of polymers and the microstructural features that are relevant to charge transport of conjugated polymers. Although the intrinsic characteristics of polymer chains impact their organization at the mesoscale and hence the morphology, the mesoscale morphology can be tuned through processing conditions.

Because a key requirement for achieving high mobility is the presence of tie chains, the length of polymer chains or the polymer molecular weight (MW) is naturally a primary parameter that critically impacts charge transport in conjugated polymers. The effect of MW on the active-layer morphology and resulting

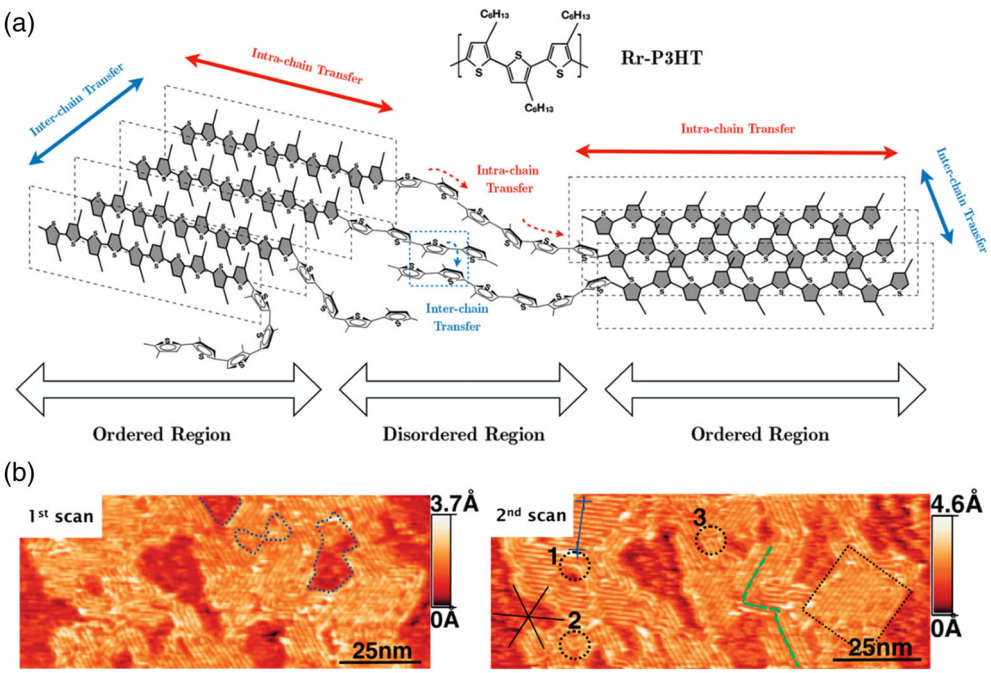

FIGURE 4 (a) Charge transport processes at different length scales in a thin film comprising edge-on regioregular P3HT (Rr-P3HT).[49] Reprinted with permission from (*Macromolecules* **2018**, *51*, 9060–9068). Copyright (2018) American Chemical Society. (b) Two scanning tunneling microscopy (STM) images of P3HT monolayer deposited on highly oriented pyrolytic graphite (HOPG), revealing its semicrystalline morphology. The contour of a chain connecting two neighboring ordered domains is underlined with a green dotted line in the second scan.[50] Adapted with permission from (*Adv. Mater.* **2003**, *15*, 881–884). Copyright (2003) John Wiley & Sons, Inc.

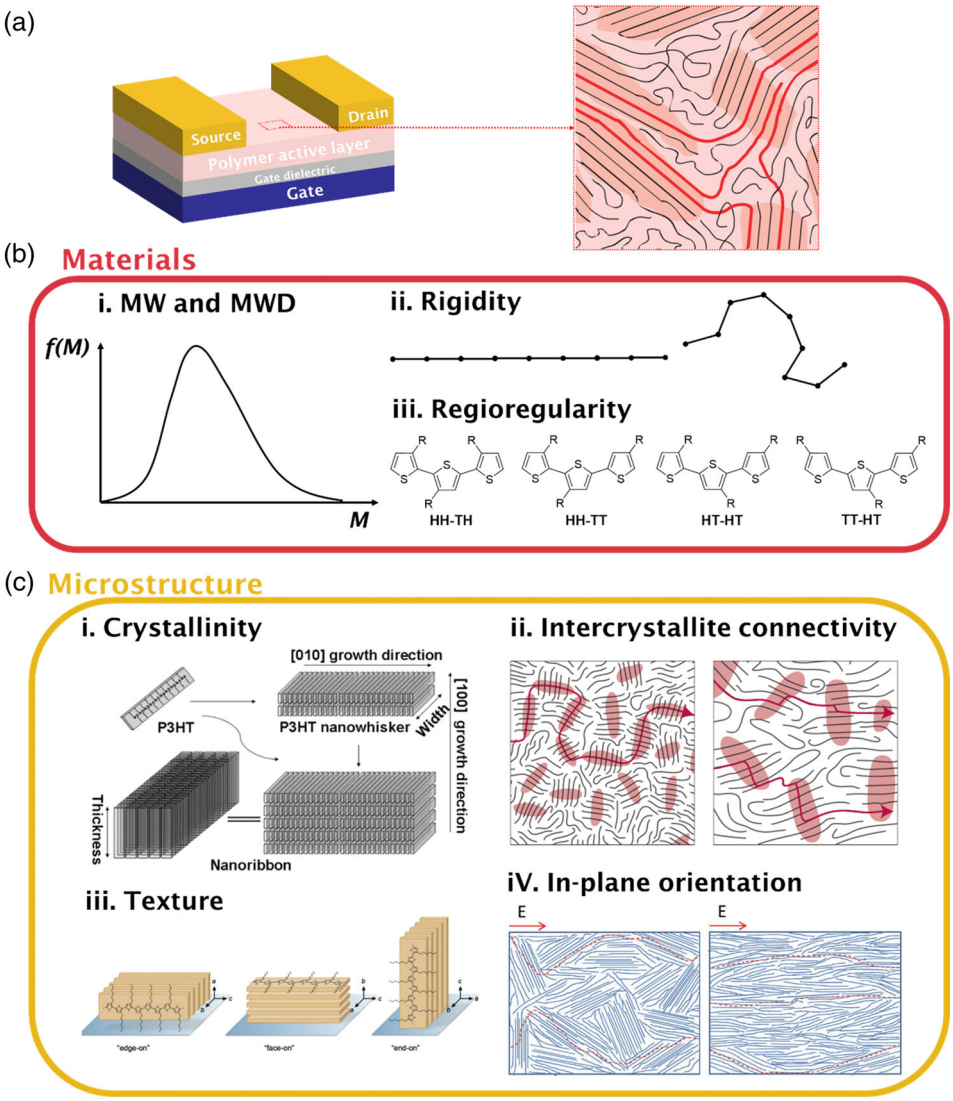

FIGURE 5 (a) A field-effect transistor in a bottom-gate, top-contact configuration. The microstructure of a semicrystalline polymer active layer is schematically shown on the right, adapted from Noriega *et al.*[15] Adapted with permission from (*Nat. Mater.* **2013**, *12*, 1038–1044). Copyright (2013) Springer Nature. (b) The important materials parameters that impact the overall morphology include: (i) molecular weight (MW) and molecular weight distribution (MWD). (ii) chain rigidity. Two chains with the same number of repeating units are schematically shown, one rod-like and the other semiflexible. (iii) regioregularity. For example, 3-alkylthiophene has four possible regioisomeric triad structures.[51] H (alkyl group R at the head position) and T (alkyl group R at the tail position).[51] (c) The important structural parameters that can be independently tuned by processing conditions include: (i) crystallinity. Nanoscale single-crystalline P3HT study has proposed the formation of P3HT nanowhiskers and nanoribbons.[52] Reprinted with permission from (*Macromolecules* **2009**, *42*, 9390–9393). Copyright (2009) American Chemical Society. (ii) Intercrystallite connectivity. The two schemes show semicrystalline films with small isolated ordered domains and interconnected ordered domains, respectively.[53] Reprinted with permission from (*Nat. Mater.* **2013**, *12*, 947–948). Copyright (2013) Springer Nature. (iii) Texture or the out-of-plane orientation of crystallites. The example shows three representative textures of P3HT crystallites: edge-on; face-on, also referred to as plane-on or flat-on; and end-on or chain-on.[54] Reprinted with permission from (*Polymer (Guildf).* **2015**, *59*, A1–A15). Copyright (2015) Elsevier Ltd. (iv) In-plane orientation. The semicrystalline films are normally isotropic in-plane but the crystalline domains can be aligned with various special techniques. The two schemes illustrate semicrystalline films with non-orientated domains and oriented domains, respectively.[55] Reprinted with permission from (*Adv. Mater.* **2018**, *1705463*, 1–34). Copyright (2018) John Wiley & Sons, Inc.

device performance of thin-film transistors comprising P3HT have been studied extensively.[56–61] There are multiple ways to represent the ensemble-average MW, most commonly, the number-average molecular weight (M_n) and weight-average molecular weight (M_w). Although the absolute mobilities of thin-film transistors differ depending on the regioregularity of the polymer semiconductors, the processing conditions employed, and so on, the mobilities of P3HT transistors generally rises

with increases in the average MWs, until they level off at threshold MWs that vary from study to study. Similar trends have been reported for other conjugated polymers, including poly(3,3″-dioctyl-2,2′:5′,2″-terthiophene), or PDOTT,[62] poly[2,6-(4,4-bis-alkyl-4*H*-cyclopenta-[2,1-*b*;3,4-*b*′]-dithiophene)-*alt*-4,7-(2,1,3-benzothiadiazole)], or CDT-BTZ copolymers,[63] and poly(2,5-bis(3-alkylthiophen-2-yl)thieno-[3,2b]thiophene), or PBTTT,[64] and so on. The initial increase in mobility is often attributed to an increase in tie-chain content as a result of increasing populations of chains that are long enough to provide electrically connective pathways between crystalline domains.[15,56,57,61] In stark contrast to the strong-MW dependence of macroscopic mobility measured by field-effect transistors, the weak MW-dependence of local intra-grain mobility measured by pulse-radiolysis time-resolved microwave conductivity (PR-TRMC) provides evidence that charge transport through amorphous regions in low-MW polymers limits macroscopic mobility in transistors and highlights the importance of intercrystallite tie chains in high-MW counterparts.[65] The mobility subsequently plateaus beyond a critical MW, presumably after the formation of the fully percolated network that can support macroscopic charge transport.[15,56,57,61] Although this percolation threshold has typically been reported to be 20–30 kg mol^{-1} for P3HT,[60,61,66] this threshold MW has varied from study to study, and as an ensemble average, it does not speak to variations in the molecular weight distribution (MWD). The convolution of MW and MWD has especially challenged the interpretation of how chain length impacts charge transport as conjugated polymers—typically made by condensation reactions—often exhibit broad MWDs.[2] To deconvolute, researchers have started to use specialized polymerization schemes[67,68] or post-synthesis fractionation[46,58,69] to obtain polymers with narrow MWDs. Blending of polymers with controlled and narrow MWD offer subsequent opportunities to systematically vary and probe the effects of MWD on charge transport. As these synthetic and post-synthetic schemes of separation are specific to polymer chemistries and have predominantly been developed for P3HT, systematic studies on the impact of MW and MWD have thus largely been limited to these model polymers and their blends.[64,69,70] Himmelberger *et al*., for example, blended low-MW P3HT (M_n of 8 kg mol^{-1}) with three different high-MW P3HTs (M_n of 29, 42, 61 kg mol^{-1}, respectively, each having a polydispersity index of 1.2) to access a unique MWD in each blending experiment, as a proxy to accessing different tie-chain content.[69] Although the mobility data qualitatively agree with the notion that more tie chains are formed with increasing fraction of the high-MW P3HT in each blend, the extent of intercrystallite connectivity was not determined. To gain insight on quantitative relationships between MW and tie-chain fraction, Duong *et al*. first used time-dependent X-ray diffraction and UV-vis absorption spectroscopy to examine the crystallization kinetics of P3EHT; they demonstrated that electrical percolation in P3EHT occurs when the interaggregate separation is on the order of the polymer chain persistence length.[31] Gu *et al*. applied the Huang-Brown model,[19,71] a framework initially used to describe the structural origins of mechanical properties in polyethylene, to quantitatively elucidate the effect of tie chains on charge transport in P3HT.[21] The Huang-Brown model assumes that polymer chains with end-to-end distances greater than, or equal to, the distance between adjacent crystallites will form tie chains.[19,71] A critical tie-chain fraction of 10^{-3}, shown in Figure 6, is required to support macroscopic charge transport, below which intercrystallite connectivity limits charge transport, and above which intracrystallite paracrystalline disorder is the bottleneck. For a polymer chain of a given MW (hence a given contour length), the polymer persistence length dictates the span of the chain, and whether it is long enough to bridge the crystalline domains that are separated by a critical distance. This work again points out that quantitative understanding of chain rigidity, alongside the mesoscale structure, is crucial for the investigation of factors that governs charge-transport properties. Further highlighting the importance of intercrystallite connectivity, Zhao *et al*. created a non-conjugated polymer, DPP-C3, by placing a propyl spacer along the backbone in the repeat unit of a conjugated diketopyrrolopyrrole (DPP)-based polymer, DPP-C0.[72] In the absence of intrachain transport, DPP-C3 transistors exhibit a low mobility of 0.009 cm^2 V^{-1} s^{-1}, but the incorporation of as little as 1 wt % of the conjugated counterpart, DPP-C0, provides the essential connectivity between crystallites and improves the mobility of transistors by nearly two orders of magnitude to 0.81 cm^2 V^{-1} s^{-1}. These results demonstrate that long polymer chains with effective conjugation along their backbone can provide the necessary electrically connective pathways between domains.[72]

More recently, copolymers with alternating donor–acceptor structure along the backbone have garnered significant interest because, intriguingly, transistors comprising them exhibit high mobilities above 1 cm^2 V^{-1} s^{-1} despite the absence of long-range order.[63,73] Notable examples include the aforementioned IDTBT, which has significantly weaker long-range order than P3HT as evidenced by X-ray diffraction, but transistors comprising IDTBT exhibit mobilities up to 3.6 cm^2 V^{-1} s^{-1}.[14]

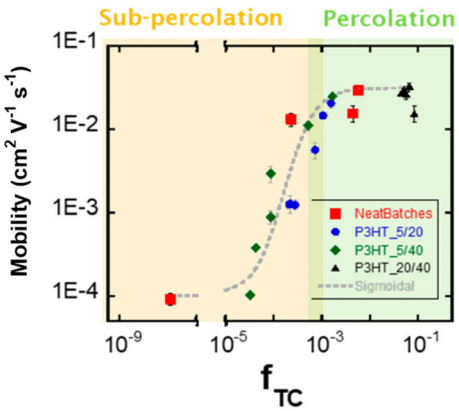

FIGURE 6 Field-effect mobility of transistors comprising P3HT blends (each having a unique MWD), as a function of the tie-chain fraction (f_{TC}). A sigmoidal line was added for visual guide.[21] Reprinted with permission from (*ACS Macro Lett*. **2018**, *7*, 1333–1338, https://pubs.acs.org/doi/10.1021/acsmacrolett.8b00626). Copyright (2018) American Chemical Society.

These findings initially seem to challenge the picture for charge transport that had been constructed based on conventional polythiophene derivatives. But subsequent understanding reveals that these donor–acceptor polymers form aggregates that can provide the short-range order and their rigid polymer backbones facilitate the interconnection between these aggregates, allowing for efficient local intermolecular hopping. The unifying requirement for efficient macroscopic charge transport thus still appears to be connectivity between ordered domains, be it between neighboring crystallites in materials that possess long-range order, or aggregates in those that only exhibit short-range order.[15,74] In the absence of aggregates or crystallites, charge transport in truly amorphous conjugated polymers is limited by slow interchain hopping, an inefficient process that is subjected to large activation energies.[15]

It is widely acknowledged that the morphology of conjugated polymers strongly depends on the conditions with which they are processed. Hence, microstructural parameters can be tuned *via* processing conditions to optimize the morphology for macroscopic charge transport. Foremost, much work has been done to grow single crystals of conjugated polymers. Merlo *et al*. first grew nanofibers of P3HT by precipitation from *p*-xylene solution. These fibers resulted in field-effect transistors with mobilities up to 0.06 $cm^2\ V^{-1}\ s^{-1}$.[75,76] Intriguingly, the average mobility (~ 0.02 $cm^2\ V^{-1}\ s^{-1}$) of such nanofiber-based transistors along the π-stacking direction is not significantly higher than that of transistors comprising drop-cast semicrystalline P3HT films that are percolated.[21] This comparison serves as indirect evidence for the assertion that once tie chains offer intercrystallite transport routes, macroscopic charge transport is limited by interchain hopping along the π-stacks within crystallites.[15,21] Many other methods have been used to produce nanoscale single crystals of P3HT,[77] including spin-coating under controlled solvent vapor pressure,[78] directional epitaxial solidification,[66] and controlled cooling from anisole.[79] Similar mobilities at 0.02 $cm^2\ V^{-1}\ s^{-1}$ was achieved for transistors comprising such single-crystalline P3HT fibers.[76,78] These single-crystal studies provide important insights on understanding intracrystallite charge transport. Yet, the mobilities of such single-crystalline fiber-based transistors are not drastically different from those comprising polycrystalline P3HT. That the mobility of P3HT transistors maxes out speaks to the quality of crystallites limiting charge transport beyond percolation and suggests improving intracrystallite order as a means to further optimize charge transport. For example, Clark *et al*. investigated the optical absorbance spectra of P3HT films that were spin-coated from a variety of solvents; they found films spun from solvents with high boiling points to generally exhibit a higher fraction of aggregates, as calculated by a weakly interacting H-aggregate model, with these aggregates exhibiting better intrachain order (smaller free exciton bandwidth) compared to those in films spin-coated from solvents with low boiling temperatures. This improved ordering within crystallites in turn leads to improved charge transport (up to one order of magnitude increase in mobility from ~10^{-3} to ~10^{-2} $cm^2\ V^{-1}\ s^{-1}$), as quantified by the field-effective mobility of transistors comprising such active layers.[80] We note that this study implicitly assumed a constant tie-chain fraction, even for films that were processed differently. It is, however, unlikely for the tie-chain content to be invariant because processing conditions will alter the crystallinity and crystallite size. The dependence of tie-chain fraction on processing conditions should be an important subject for future studies; therefore, we can better assess the dominant structural parameter that governs charge transport.

There is also a correlation between charge transport and the crystalline texture, that is, the out-of-plane orientation of crystallites with respect to the substrate. Sirringhaus *et al*. initially demonstrated access to different crystallite orientations by altering the regioregularity of P3HT and the casting method; transistors comprising P3HT crystallites that are preferentially oriented edge-on exhibit mobilities that are three orders of magnitude higher than those with crystallites that are preferentially oriented face-on.[32] There exist, however, studies that contradict the simplistic picture that lateral in-plane charge transport is most favorable when crystallites are preferentially oriented edge-on. O'Connor *et al*. showed mechanically straining P3HT thin films to improve the mobility along the strain direction despite inducing a higher population of face-on crystallites.[81] And transistors comprising predominantly face-on oriented poly{[*N*,*N*-9-bis(2-octyldodecyl)-naphthalene-1,4,5,8-bis(dicarboximide)-2,6-diyl]-*alt*-5,59-(2,29-bithiophene)}, or P(NDI2OD-T2), have been reported to exhibit electron mobilities as high as 0.18 $cm^2\ V^{-1}\ s^{-1}$.[82] These exceptions point to the complexities of how mesoscale structure impacts charge transport. The authors attributed the unconventional efficient transport in this largely face-on oriented polymer to enhanced hopping through the small fraction of out-of-plane π-stacks in connected domains.

Although the effect of out-of-plane orientation of crystallites on charge transport may be second-order to domain connectivity, the in-plane orientation of crystallites plays a more significant role.[83] A substantial boost in mobility can come from uniaxially aligning conjugated polymers to promote preferential in-plane orientation of the polymer backbone, thereby facilitating efficient charge transport in the direction of alignment.[55] In fact, almost all record-breaking mobilities have resulted from transistors comprising conjugated polymers that have been uniaxially aligned. For instance, transistors comprising spin-cast poly[4-(4,4-dihexadecyl-4*H*-cyclopenta [1,2-*b*:5,4-*b*′]dithiophen-2-yl)-*alt*-[1,2,5]-thiadiazolo[3,4-*c*]pyridine], or PCDTPT, exhibit a mobility of 0.6 $cm^2\ V^{-1}\ s^{-1}$,[84] but those comprising nanogroove-aligned PCDTPT exhibited mobilities above 10 $cm^2\ V^{-1}\ s^{-1}$, highlighting the crucial role of in-plane orientation on charge transport.[9,10] A wide array of other techniques have been developed to induce preferential alignment of conjugated polymers to improve charge transport, as nicely summarized in the recent review by Khim *et al*.[55] Macroscopic charge-transport enhancement along the alignment direction can arise from changes in the properties of the crystallites, grain boundaries, or intercrystalline amorphous regions.[81,85] Although changes to the crystallite properties can be probed directly using a suite of structural characterization tools, changes to the amorphous regions are

much more challenging to assess.[86,87] By demonstrating a much higher macroscopic charge-transport anisotropy than the local charge-transport anisotropy in highly strain-aligned P3HT, for example, O'Connor *et al*. argued that the overall improved charge transport along the alignment direction can be attributed to favorably aligned tie chains in the amorphous regions that connect the well-oriented aggregates.[86] This study highlights the critical role of polymer tie chains on charge transport in these semicrystalline films, as we believe, without tie chains, the crystallites, be them aligned or unaligned, would still be isolated and the macroscopic charge transport to remain limited by slow interchain hopping in the amorphous region between these crystallites.

Theoretical Studies

Building upon the progress on experimental work, our understanding of charge transport in conjugated polymers has also benefitted from contributions from theoretical studies. Predictive models of charge-transport processes have provided insights on the complex structure–property relationships, enabling, to first order, the rational design of conjugated polymers.[41,88] However, it remains challenging to develop theoretical models that can simultaneously capture the intricacies of local molecular structure and mesoscale morphology. Most of the theoretical studies in the literature have focused on either the microscopic picture or have coarse-grained the microscopic; therefore, they can address the mesoscale structure.[49]

Although the coarse-grained macroscopic models have an advantage of being much less computationally taxing, they cannot capture the microstructural details of semiconducting polymers needed for understanding charge transport. For instance, the widely used Gaussian disorder model (GDM),[89,90] which describes a 3D material as a spatially and energetically disordered grid of sites, does not distinguish intrachain and interchain transport and has a spatial resolution that is comparable to typical device dimensions.[41,49] Although GDM is able to explain observations, like the electric-field dependence of charge mobility, it lacks sufficient microstructural details to fully shed light on such heterogeneous systems. In an attempt to capture additional detail, Noriega *et al*. reported a transport model that incorporates individual polymer chain conformations.[35] Their results provide a theoretical basis for charge transport across multiple scales: at short distances, charges move most efficiently along the polymer backbone, and at longer distances, charge transport occurs with multiple interchain hops, reducing the effective rate of charge transport.[35]

Mollinger *et al*. extended the framework developed by Noriega *et al*. for amorphous polymers to investigate semicrystalline polymers and provided a direct connection between microstructure and charge transport under an external field.[41] Shown in Figure 7a, the polymer thin film is approximated in two-dimensions with circular crystallites evenly distributed on a triangular lattice having a center-to-center spacing, *s*, and an edge-to-edge spacing, *d*. In this scheme, two paths for intercrystallite charge transport are highlighted; Path 1 in which charge travels along the polymer tie chain between two crystallites, and Path 2 in which charge transport takes place through interchain hopping. With WLC-generated polymer chain conformations, the authors modeled charge transport using dynamic Monte Carlo simulations, with μ_{chain}, μ_{hop}, and $\mu_{crystal}$ describing on-chain mobility, inter-chain mobility in the amorphous regions, and an intra-crystallite mobility that is averaged over all chain orientations, respectively. Figure 7b shows the time-dependent mobility for semicrystalline films with crystallite fractions (f) varying from 0 to 0.9, visualizing the multiscale nature of charge transport. In these simulations, the long (microsecond) and short (picosecond) time scales essentially correspond to the respective long (micrometer) and short (Ångstrom) length scales of interest. In the case of an amorphous film (f = 0.0), intrachain transport occurs with μ_{chain} at short distances (Ångstrom) while interchain hopping, with a corresponding mobility of μ_{hop}, dominates over much longer distances (micrometer). At intermediate distances (~ 1–10 nm), $\mu_{crystal}$ dominate in semicrystalline films. For highly crystalline films, transport is largely determined by

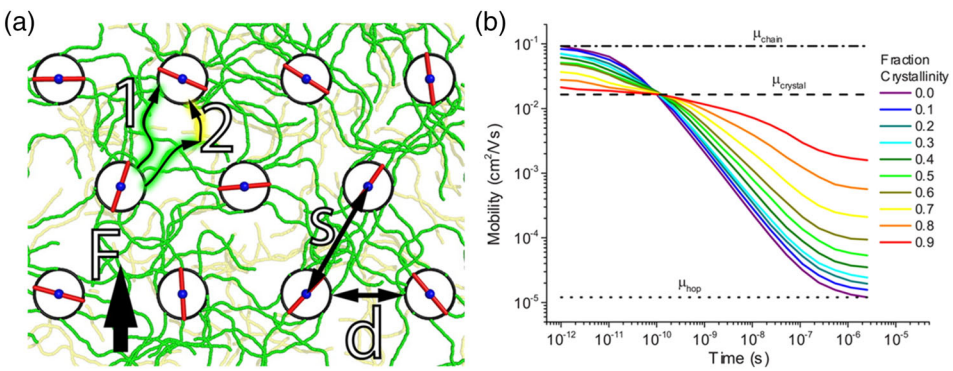

FIGURE 7 (a) Schematic representation of the 2D model developed by Mollinger *et al*. showing an array of crystallites arranged on a triangular lattice. (b) Multiscale mobility for different areal coverage of crystallites. Three relevant mobility values are evident, with μ_{chain}, μ_{hop}, and $\mu_{crystal}$ describing on-chain mobility, inter-chain mobility in the amorphous regions, and an intra-crystallite mobility that is averaged over all chain orientations, respectively.[41] Reprinted with permission from (*ACS Macro Lett*. **2015**, *4*, 708–712). Copyright (2015) American Chemical Society.

$\mu_{crystal}$. The outcome of this model is consistent with prior experimental work that pointed to the importance of a percolative network of crystallites formed with tie chains to support macroscopic charge transport. Consistent with the extended Huang-Brown model reported by Gu *et al*., this model also highlights how an analytical understanding of chain conformations allows subsequent determination of the statistical probability of forming tie chains and, accordingly, the percolation threshold. This predictive model has also been used to rationalize experimentally observed trend in mobility as a function of MW.[91] Segatta *et al*. further introduced a mesoscopic model with control over additional morphological details that simultaneously considers single-chain characteristics and the global semicrystalline morphology, the results of which again confirm the importance of interconnected crystallites for efficient macroscopic charge transport.[49] Recent work by Jankowski *et al*. with more sophisticated theorectical treatments, in which they combined the large simulation volumes from optimized molecular dynamics (MD) simulations of P3HT with quantum chemical calculations (QCC)-informed charge transport, further bolsters the critical role of tie-chain connectivity in charge transport.[92,93]

Theoretical efforts have shed light on our understanding of charge transport at different length scales and confirmed the importance of the interconnection between crystallites. Considering existing experimental results and ongoing experiments, future theoretical studies should incorporate the effects of crystallite orientation to assess the relative importance of these structural parameters on charge transport.

OPPORTUNITIES FOR IMPROVING CHARGE TRANSPORT

Although the effect of microstructure on charge transport is multifaceted and cannot be easily reduced to a single universal parameter,[94] our collective mechanistic understanding from both experimental and theoretical studies has pointed to the importance of interconnected ordered domains. This necessity is uniquely attributable to the macromolecular nature of conjugated polymers. Unique to polymeric semiconductors and not found in molecular semiconductors are thus efficient intrachain transport that is faster intermolecular hopping and electrical connectivity between ordered domains facilitated by the presence of polymer tie chains. Optimization that leverages this criterion to improve macroscopic charge transport can be broadly grouped into three main categories.

Leverage the Macromolecular Nature of Conjugated Polymers to Promote Favorable Intrachain Transport

High-performance polymers should have rigid backbones without significant torsion. Present high-performance donor–acceptor polymers typically have persistence length on the order of 10 nm or above, compared to the persistence length of P3HT at 3 nm.[28] The benefits of backbone rigidity have been particularly demonstrated with IDTBT copolymers. Transistors having mobilities as high as 3.6 $cm^2\ V^{-1}\ s^{-1}$ has been attributed to its rigid and torsion-free backbone.[14,48] Simulation results show that mechanical stretching can also rigidify polymer chains, increasing the effective persistence length and leading to higher-yet overall conductivities.[35] Post-synthesis chain alignment strategies should thus be used in conjunction with rigid conjugated polymers to further reduce intrachain defects and align polymer chains and crystallites to enable the most efficient intrachain charge transport.[9,10,81,95]

Establish Connectivity Between Ordered Domains to Bypass Charge-Transport Barriers in Amorphous Regions

To avoid inefficient interchain hopping in the amorphous regions of conjugated polymers, connections between adjacent ordered domains by polymer tie chains are indispensable. The formation of such physical connections depends on the polymer chain contour length, the polymer chain persistence length, and the characteristic spacing between neighboring ordered regions.[21] For such purposes, polymers with high MWs[15,63,96] and high crystallinity[97–99] are needed. And, as described above, polymers with rigid coplanar backbones have higher persistence length, which should in turn also facilitate the formation of tie chains.[21]

Enhance Interchain Coupling to Improve Local Hopping

Because typical device dimensions are much larger than the polymer chain length, macroscopic charge transport inevitably involves numerous hopping events between polymer chains. In the percolated network of a conjugated polymer, charge transport is ultimately limited by interchain transport within ordered domains.[15,21] Hence, the overall charge transport can be improved by enhancing local interchain coupling. The aforementioned backbone planarity is also beneficial to enhancing interchain transport, because the less-twisted polymer chains can π-stack more readily and improve the interchain ordering.[96,100] Side chains, although primarily used as solubilizing groups, can be commonly engineered to modulate the π–π stacking distance to improve local packing.[96,101] Mei *et al*. replaced branched alkyl side chains with less sterically-hindered siloxane-terminated side chains in a isoindigo-based polymer. This chemical substitution of the side chain led to a nearly 5% reduction in the π-stacking distance and more than six times higher in transistor mobility to 2.0 $cm^2\ V^{-1}\ s^{-1}$.[73] Kang *et al*. moved the side-chain branch point away from the backbone in a DPP-based polymer, enabling a 3% reduction in the π-stacking distance and stronger intermolecular packing.[102] This small structural change led to an almost 10-fold increase in transistor mobility to 9.8 $cm^2\ V^{-1}\ s^{-1}$. Similarly, Bridges *et al*. systematically shortened the π-stacking distance in cyclopentadithiophene-benzothiadiazole copolymers by moving the branch point further away from the conjugated backbone.[103] As the π-stacking distance decreases from 3.8 to 3.5 Å, the mobility of the resulting transistor increases from $\sim 10^{-4}$ to 0.4 $cm^2\ V^{-1}\ s^{-1}$. Another way to tune interchain interactions is through heteroatom substitution.[104,105] With a series of naphthalenediimide-based copolymers, Zhao *et al*. demonstrated that selenophene heterocycles endow closer π–π stacking distances of the conjugated core than the thiophene-containing counterparts, leading to a mobility of 7.8 $cm^2\ V^{-1}\ s^{-1}$, three times higher than that exhibited by transistors comprising the thiophene copolymers.[106]

CONCLUSIONS AND OUTLOOK

In this review, we have described the multiscale scheme of charge transport in conjugated polymers and proposed strategies for its improvement. Continuous progress in both experiments and theories has partially addressed the key challenges of linking molecular characteristics of conjugated polymers with their macroscopic properties. Classical polymer physics, often overlooked in the field of polymer transistors, may provide the missing pieces for solving the puzzles presented by such structurally heterogenous materials. Summarizing structure–property relationships, we assert that the presence of interconnected ordered domains is a key to optimizing charge transport in conjugated polymers. Based on this general principle, we recommend three strategies for improving charge transport in conjugated polymers: promote intrachain transport, establish intercrystallite connectivity, and enhance interchain coupling.

With improved predictions for mesoscale ordering given molecular structure and chain characteristics, we hope to one day be able to specify *a priori*, and design accordingly, chemical structures and processing conditions to achieve the optimal structure and ordering over multiple length scales for efficient charge transport. Coupled with proper device engineering on other transistor parameters, like channel length and contact resistance,[107] continual developments of new materials and refinement of our understanding of them should lead to steady increases in the performance of polymer transistors, realizing their potential in applications, like displays and sensors, that have demanding performance requirements.

ACKNOWLEDGMENTS

This work was supported by ExxonMobil through its membership in the Princeton E-ffiliates Partnership of the Andlinger Center for Energy and the Environment. K.G. acknowledges the Mr. and Mrs. Yan Huo *94*95 Graduate Fellowship, administered by Princeton Institute for International and Regional Studies (PIIRS). Y.-L.L. acknowledges partial funding from the National Science Foundation through grant CMMI-1824674.

REFERENCES AND NOTES

1 Y.-L. Loo, I. Mcculloch, *MRS Bull.* **2008**, *33*, 653.

2 A. Facchetti, *Chem. Mater.* **2011**, *23*, 733.

3 S. Holliday, J. E. Donaghey, I. McCulloch, *Chem. Mater.* **2014**, *26*, 647.

4 X. Guo, Y. Xu, S. Ogier, T. N. Ng, M. Caironi, A. Perinot, L. Li, J. Zhao, W. Tang, R. A. Sporea, A. Nejim, J. Carrabina, P. Cain, F. Yan, *IEEE Trans. Electron Devices* **2017**, *64*, 1906.

5 A. Tsumura, H. Koezuka, T. Ando, *Appl. Phys. Lett.* **1986**, *49*, 1210.

6 S. Wang, M. Kappl, I. Liebewirth, M. Müller, K. Kirchhoff, W. Pisula, K. Müllen, *Adv. Mater.* **2012**, *24*, 417.

7 J. Li, Y. Zhao, H. S. Tan, Y. Guo, C. A. Di, G. Yu, Y. Liu, M. Lin, S. H. Lim, Y. Zhou, H. Su, B. S. Ong, *Sci. Rep.* **2012**, *2*, 1.

8 G. Kim, S. J. Kang, G. K. Dutta, Y. K. Han, T. J. Shin, Y. Y. Noh, C. Yang, *J. Am. Chem. Soc.* **2014**, *136*, 9477.

9 H. R. Tseng, H. Phan, C. Luo, M. Wang, L. A. Perez, S. N. Patel, L. Ying, E. J. Kramer, T. Q. Nguyen, G. C. Bazan, A. J. Heeger, *Adv. Mater.* **2014**, *26*, 2993.

10 C. Luo, A. Ko, K. Kyaw, L. A. Perez, S. Patel, M. Wang, B. Grimm, G. C. Bazan, E. J. Kramer, A. J. Heeger, *Nano Lett.* **2014**, *14*, 2764.

11 Y. Yamashita, F. Hinkel, T. Marszalek, W. Zajaczkowski, W. Pisula, M. Baumgarten, H. Matsui, K. Müllen, J. Takeya, *Chem. Mater.* **2016**, *28*, 420.

12 Z. Bao, A. Dodabalapur, A. J. Lovinger, *Appl. Phys. Lett.* **1996**, *69*, 4108.

13 I. McCulloch, M. Heeney, C. Bailey, K. Genevicius, I. MacDonald, M. Shkunov, D. Sparrowe, S. Tierney, R. Wagner, W. Zhang, M. L. Chabinyc, R. J. Kline, M. D. McGehee, M. F. Toney, *Nat. Mater.* **2006**, *5*, 328.

14 X. Zhang, H. Bronstein, A. J. Kronemeijer, J. Smith, Y. Kim, R. J. Kline, L. J. Richter, T. D. Anthopoulos, H. Sirringhaus, K. Song, M. Heeney, W. Zhang, I. McCulloch, D. M. DeLongchamp, *Nat. Commun.* **2013**, *4*, 2238.

15 R. Noriega, J. Rivnay, K. Vandewal, F. P. V. Koch, N. Stingelin, P. Smith, M. F. Toney, A. Salleo, *Nat. Mater.* **2013**, *12*, 1038.

16 G. Strobl, *The physics of polymers*, 3rd ed.; Springer-Verlag Berlin Heidelberg, **2007**.

17 R. Xie, R. H. Colby, E. D. Gomez, *Adv. Electron. Mater.* **2018**, *4*, 1700356.

18 B. O'Connor, E. P. Chan, C. Chan, B. R. Conrad, L. J. Richter, R. J. Kline, M. Heeney, I. McCulloch, C. L. Soles, D. M. DeLongchamp, *ACS Nano* **2010**, *4*, 7538.

19 Y.-L. Huang, N. Brown, *J. Mater. Sci.* **1988**, *23*, 3648.

20 R. Seguela, *J. Polym. Sci. Part B Polym. Phys.* **2005**, *43*, 1729.

21 K. Gu, C. R. Snyder, J. Onorato, C. K. Luscombe, A. W. Bosse, Y.-L. Loo, *ACS Macro Lett.* **2018**, *7*, 1333.

22 B. McCulloch, V. Ho, M. Hoarfrost, C. Stanley, C. Do, W. T. Heller, R. A. Segalman, *Macromolecules* **2013**, *46*, 1899.

23 M. Brinkmann, J.-C. Wittmann, *Adv. Mater.* **2006**, *18*, 860.

24 F. P. V. Koch, M. Heeney, P. Smith, *J. Am. Chem. Soc.* **2013**, *135*, 13699.

25 C. R. Snyder, R. C. Nieuwendaal, D. M. DeLongchamp, C. K. Luscombe, P. Sista, S. D. Boyd, *Macromolecules* **2014**, *47*, 3942.

26 A. D. Scaccabarozzi, N. Stingelin, *J. Mater. Chem. A* **2014**, *2*, 10818.

27 Y. Lee, E. D. Gomez, *Macromolecules* **2015**, *48*, 7385.

28 B. Kuei, E. D. Gomez, *Soft Matter* **2017**, *13*, 49.

29 R. Noriega, *Macromol. Rapid Commun.* **2018**, *39*, 1.

30 D. T. Duong, M. F. Toney, A. Salleo, *Phys. Rev. B Condens. Matter Mater. Phys.* **2012**, *86*, 1.

31 D. T. Duong, V. Ho, Z. Shang, S. Mollinger, S. C. B. Mannsfeld, J. Dacuna, M. F. Toney, R. Segalman, A. Salleo, *Adv. Funct. Mater.* **2014**, *24*, 4515.

32 H. Sirringhaus, P. J. Brown, R. H. Friend, M. M. Nielsen, K. Bechgaard, B. M. W. Langeveld-Voss, a. J. H. Spiering, R. a. J. Janssen, E. W. Meijer, P. Herwig, D. M. de Leeuw, *Nature* **1999**, *401*, 685.

33 A. Salleo, *Mater. Today* **2007**, *10*, 38.

34 F. Laquai, G. Wegner, H. Bässler, *Philos. Trans. R. Soc. A Math. Phys. Eng. Sci.* **2007**, *365*, 1473.

35 R. Noriega, A. Salleo, A. J. Spakowitz, *Proc. Natl. Acad. Sci. U. S. A.* **2013**, *110*, 16315.

36 J. Rivnay, S. C. B. Mannsfeld, C. E. Miller, A. Salleo, M. F. Toney, *Chem. Rev.* **2012**, *112*, 5488.

37 H. Dong, W. Hu, *Acc. Chem. Res.* **2016**, *49*, 2435.

38 Z. G. Wang, *Macromolecules* **2017**, *50*, 9073.

39 B. J. Schwartz, *Annu. Rev. Phys. Chem.* **2003**, *54*, 141.

40 Z. Hu, T. Adachi, Y. G. Lee, R. T. Haws, B. Hanson, R. J. Ono, C. W. Bielawski, V. Ganesan, P. J. Rossky, D. A. Vanden Bout, *ChemPhysChem* **2013**, *14*, 4143.

41 S. A. Mollinger, B. A. Krajina, R. Noriega, A. Salleo, A. J. Spakowitz, *ACS Macro Lett.* **2015**, *4*, 708.

42 M. Rubinstein, R. R. H. Colby, *Polymer physics*, 1st ed.; Oxford University Press: New York, **2003**.

43 W. Zhang, E. D. Gomez, S. T. Milner, *Macromolecules* **2014**, *47*, 6453.

44 G. W. Heffner, D. S. Pearson, *Macromolecules* **1991**, *24*, 6295.

45 G. Fytas, H. G. Nothofer, U. Scherf, D. Vlassopoulos, *Macromolecules* **2002**, *35*, 481.

46 K. Gu, J. Onorato, S. S. Xiao, C. K. Luscombe, Y.-L. Loo, *Chem. Mater.* **2018**, *30*, 570.

47 B. L. Farmer, B. R. Chapman, D. S. Dudis, W. W. Adams, *Polymer* **1993**, *34*, 1588.

48 D. Venkateshvaran, M. Nikolka, A. Sadhanala, V. Lemaur, M. Zelazny, M. Kepa, M. Hurhangee, A. J. Kronemeijer, V. Pecunia, I. Nasrallah, I. Romanov, K. Broch, I. McCulloch, D. Emin, Y. Olivier, J. Cornil, D. Beljonne, H. Sirringhaus, *Nature* **2014**, *515*, 384.

49 F. Segatta, G. Lattanzi, P. Faccioli, *Macromolecules* **2018**, *51*, 9060.

50 B. Grévin, P. Rannou, R. Payerne, A. Pron, J. P. Travers, *Adv. Mater.* **2003**, *15*, 881.

51 S. Ludwigs, *P3HT revisited – from molecular scale to solar cell devices*; Springer-Verlag Berlin Heidelberg, **2014**.

52 J. Liu, M. Arif, J. Zou, S. I. Khondaker, L. Zhai, *Macromolecules* **2009**, *42*, 9390.

53 V. Podzorov, *Nat. Mater.* **2013**, *12*, 947.

54 I. Osaka, K. Takimiya, *Polymer* **2015**, *59*, A1.

55 D. Khim, A. Luzio, G. E. Bonacchini, G. Pace, M. J. Lee, Y. Y. Noh, M. Caironi, *Adv. Mater.* **2018**, *1705463*, 1.

56 R. J. Kline, M. D. McGehee, E. N. Kadnikova, J. Liu, J. M. J. Fréchet, *Adv. Mater.* **2003**, *15*, 1519.

57 R. J. Kline, M. D. McGehee, E. N. Kadnikova, J. Liu, J. M. J. Fréchet, M. F. Toney, *Macromolecules* **2005**, *38*, 3312.

58 A. Zen, J. Pflaum, S. Hirschmann, W. Zhuang, F. Jaiser, U. Asawapirom, J. P. Rabe, U. Scherf, D. Neher, *Adv. Funct. Mater.* **2004**, *14*, 757.

59 A. Zen, M. Saphiannikova, D. Neher, *Macromolecules* **2006**, *39*, 2162.

60 J. F. Chang, J. Clark, N. Zhao, H. Sirringhaus, D. W. Breiby, J. W. Andreasen, M. M. Nielsen, M. Giles, M. Heeney, I. McCulloch, *Phys. Rev. B* **2006**, *74*, 115318.

61 F. P. V. Koch, J. Rivnay, S. Foster, C. Müller, J. M. Downing, E. Buchaca-Domingo, P. Westacott, L. Yu, M. Yuan, M. Baklar, Z. Fei, C. Luscombe, M. A. McLachlan, M. Heeney, G. Rumbles, C. Silva, A. Salleo, J. Nelson, P. Smith, N. Stingelin, *Prog. Polym. Sci.* **2013**, *38*, 1978.

62 J.-M. Verilhac, R. Pokrop, G. LeBlevennec, I. Kulszewicz-Bajer, K. Buga, M. Zagorska, S. Sadki, A. Pron, *J. Phys. Chem. B* **2006**, *110*, 13305.

63 H. N. Tsao, D. M. Cho, I. Park, M. R. Hansen, A. Mavrinskiy, D. Y. Yoon, R. Graf, W. Pisula, H. W. Spiess, K. Müllen, *J. Am. Chem. Soc.* **2011**, *133*, 2605.

64 A. Gasperini, K. Sivula, *Macromolecules* **2013**, *46*, 9349.

65 P. Pingel, A. Zen, R. D. Abellón, F. C. Grozema, L. D. a. Siebbeles, D. Neher, *Adv. Funct. Mater.* **2010**, *20*, 2286.

66 M. Brinkmann, P. Rannou, *Adv. Funct. Mater.* **2007**, *17*, 101.

67 H. A. Bronstein, C. K. Luscombe, *J. Am. Chem. Soc.* **2009**, *131*, 12894.

68 S. Tamba, K. Shono, A. Sugie, A. Mori, *J. Am. Chem. Soc.* **2011**, *133*, 9700.

69 S. Himmelberger, K. Vandewal, Z. Fei, M. Heeney, A. Salleo, *Macromolecules* **2014**, *47*, 7151.

70 A. Gasperini, X. A. Jeanbourquin, K. Sivula, *J. Polym. Sci. Part B Polym. Phys.* **2016**, *54*, 2245.

71 Y. Huang, N. Brown, *J. Polym. Sci. Part B Polym. Phys.* **1991**, *29*, 129.

72 Y. Zhao, X. Zhao, M. Roders, G. Qu, Y. Diao, A. L. Ayzner, J. Mei, *Chem. Mater.* **2015**, *27*, 7164.

73 J. Mei, D. H. Kim, A. L. Ayzner, M. F. Toney, Z. Bao, *J. Am. Chem. Soc.* **2011**, *133*, 20130.

74 S. Wang, S. Fabiano, S. Himmelberger, S. Puzinas, X. Crispin, A. Salleo, M. Berggren, *Proc. Natl. Acad. Sci.* **2015**, *112*, 10599.

75 J. a. Merlo, C. D. Frisbie, *J. Polym. Sci. Part B Polym. Phys.* **2003**, *41*, 2674.

76 J. A. Merlo, C. D. Frisbie, *J. Phys. Chem. B* **2004**, *108*, 19169.

77 J. A. Lim, F. Liu, S. Ferdous, M. Muthukumar, A. L. Briseno, *Mater. Today* **2010**, *13*, 14.

78 D. H. Kim, Y. Jang, Y. D. Park, K. Cho, *J. Phys. Chem. B* **2006**, *110*, 15763.

79 S. Samitsu, T. Shimomura, S. Heike, T. Hashizume, K. Ito, *Macromolecules* **2008**, *41*, 8000.

80 J. Clark, J. F. Chang, F. C. Spano, R. H. Friend, C. Silva, *Appl. Phys. Lett.* **2009**, *94*, 2007.

81 B. O'Connor, R. J. Kline, B. R. Conrad, L. J. Richter, D. Gundlach, M. F. Toney, D. M. DeLongchamp, *Adv. Funct. Mater.* **2011**, *21*, 3697.

82 J. Rivnay, M. F. Toney, Y. Zheng, I. V. Kauvar, Z. Chen, V. Wagner, A. Facchetti, A. Salleo, *Adv. Mater.* **2010**, *22*, 4359.

83 R. Joseph Kline, M. D. McGehee, M. F. Toney, *Nat. Mater.* **2006**, *5*, 222.

84 L. Ying, B. B. Y. Hsu, H. Zhan, G. C. Welch, P. Zalar, L. A. Perez, E. J. Kramer, T. Nguyen, A. J. Heeger, W. Wong, G. C. Bazan, *J. Am. Chem. Soc.* **2011**, *133*, 18538.

85 L. H. Jimison, M. F. Toney, I. McCulloch, M. Heeney, A. Salleo, *Adv. Mater.* **2009**, *21*, 1568.

86 B. T. O'Connor, O. G. Reid, X. Zhang, R. J. Kline, L. J. Richter, D. J. Gundlach, D. M. Delongchamp, M. F. Toney, N. Kopidakis, G. Rumbles, *Adv. Funct. Mater.* **2014**, *24*, 3422.

87 D. Wu, M. Kaplan, H. W. Ro, S. Engmann, D. A. Fischer, D. M. DeLongchamp, L. J. Richter, E. Gann, L. Thomsen, C. R. McNeill, X. Zhang, *Chem. Mater.* **2018**, *30*, 1924.

88 J. Nelson, J. J. Kwiatkowski, J. Kirkpatrick, J. M. Frost, *Acc. Chem. Res.* **2009**, *42*, 1768.

89 N. T. Binh, L. Q. Minh, H. Bässler, *Synth. Met.* **1993**, *58*, 39.

90 W. F. Pasveer, J. Cottaar, C. Tanase, R. Coehoorn, P. A. Bobbert, P. W. M. Blom, M. De Leeuw, M. A. J. Michels, *Phys. Rev. Lett.* **2005**, *94*, 1.

91 S. A. Mollinger, A. Salleo, A. J. Spakowitz, *ACS Cent. Sci.* **2016**, *2*, 910.

92 E. Miller, M. Jones, M. Henry, P. Chery, K. Miller, E. Jankowski, *Polymers* **2018**, *10*, 1305.

93 E. Miller, M. Jones, E. Jankowski, *Polymers* **2018**, *10*, 1358.

94 A. Salleo, R. J. Kline, D. M. DeLongchamp, M. L. Chabinyc, *Adv. Mater.* **2010**, *22*, 3812.

95 S. Schott, E. Gann, L. Thomsen, S. H. Jung, J. K. Lee, C. R. McNeill, H. Sirringhaus, *Adv. Mater.* **2015**, *27*, 7356.

96 S. Himmelberger, A. Salleo, *MRS Commun.* **2015**, *5*, 383.

97 S. Cho, K. Lee, J. Yuen, G. Wang, D. Moses, A. J. Heeger, M. Surin, R. Lazzaroni, *J. Appl. Phys.* **2006**, *100*, 114503.

98 K. Vakhshouri, E. D. Gomez, *Macromol. Rapid Commun.* **2012**, *33*, 2133.

99 K. Vakhshouri, B. H. Smith, E. P. Chan, C. Wang, A. Salleo, C. Wang, A. Hexemer, E. D. Gomez, *Macromolecules* **2016**, *49*, 7359.

100 J. H. Carpenter, M. Ghasemi, E. Gann, I. Angunawela, S. J. Stuard, J. J. Rech, E. Ritchie, B. T. O'Connor, J. Atkin, W. You, D. M. DeLongchamp, H. Ade, *Adv. Funct. Mater.* **2019**, *29*, 1806977.

101 J. Mei, Z. Bao, *Chem. Mater.* **2014**, *26*, 604.

102 I. Kang, H. J. Yun, D. S. Chung, S. K. Kwon, Y. H. Kim, *J. Am. Chem. Soc.* **2013**, *135*, 14896.

103 C. R. Bridges, M. J. Ford, E. M. Thomas, C. Gomez, G. C. Bazan, R. A. Segalman, *Macromolecules* **2018**, *51*, 8597.

104 Z. Li, W. Zhang, L. Feng, X. Shen, Y. Mai, *Polym. Plast. Technol. Eng.* **2014**, *53*, 1194.

105 W. Zhang, Y. Liu, G. Yu, *Adv. Mater.* **2014**, *26*, 6898.

106 Z. Zhao, Z. Yin, H. Chen, L. Zheng, C. Zhu, L. Zhang, S. Tan, H. Wang, Y. Guo, Q. Tang, Y. Liu, *Adv. Mater.* **2017**, *29*, 1602410.

107 H. Klauk, *Adv. Electron. Mater.* **2018**, *4*, 1.